치의학박사학위논문

Development and evaluation of navigation system for dental implant surgery completed in all-in-one visit

즉시 적용 가능한 치과 임플란트 수술용

영상유도 수술 시스템의 개발 및 평가

2014년 2월

서울대학교 대학원

치의과학과 구강악안면방사선학전공

김 성 구

Development and evaluation of navigation system for dental implant surgery completed in all-in-one visit

지도 교수 이 원 진

이 논문을 치의학박사 학위논문으로 제출함
2013년 10월

서울대학교 대학원
치의과학과 구강악안면방사선학 전공
김 성 구

김성구의 치의학박사 학위논문을 인준함
2013년 12월

위 원 장 _____ (인)

부위원장 _____ (인)

위 원 _____ (인)

위 원 _____ (인)

위 원 _____ (인)

Abstract

Development and evaluation of navigation system for dental implant surgery completed in all-in-one visit

Sung-Goo Kim, DDS, MSD

Department of Oral and Maxillofacial Radiology

The Graduate School

Seoul National University

Purpose: In this study, we have developed a new image guided navigation system for dental implant using cone-beam computed tomography image, and evaluated its accuracy.

Materials and methods: Image guided navigation system based on an optical tracking camera was developed. In the developed system, new instrument tracking tool and patient tracking tool were applied. A patient-specific splint was improvised using a bite splint and dental impression material. Also, registration method using pre-recorded fiducials and direct offset determination method were developed. Accuracy of these registration and direct offset determination methods was measured through target registration errors (TRE) of 10 ceramic spheres. To

measure error of the image guided navigation system for placed implants, the 110 implants were actually installed, and the accuracy of the developed system was evaluated.

Results: The total mean (± SD) TRE of newly developed system was 0.35 ± 0.11 mm. After registration by pre-recorded fiducials, the mean TRE was 0.34 ± 0.18 mm. The offset for a random drill was directly calibrated, and then by using it, a mean TRE was 0.35 ± 0.16 mm as a result. There was no significant difference ($P > 0.05$) in accuracy among registration methods and direct offset determination. The total mean error between 110 planned implants and the actually placed implants was 0.41 ± 0.12 mm at the center point of platform, 0.56 ± 0.14 mm at the center point of apex, and 2.64 ± 1.31 ° was the angular deviation of the long axis of the implant.

Conclusion: A new image guided navigation system based on CBCT images for dental implant was developed to overcome some disadvantages of the conventional method, and the accuracy of the developed system was proved to be sufficiently high for clinical application. It will be possible to perform a dental implant surgery in all-in-one visit by using the developed image guided navigation system.

Keywords: Image-Guided Surgery; Navigation Surgery; Dental Implants; Cone-Beam Computed Tomography; All-in-one visit Surgery

Student Number: 2008-31042

Development and evaluation of navigation system for dental implant surgery completed in all-in-one visit

Sung-Goo Kim, DDS, MSD

Department of Oral and Maxillofacial Radiology,

Graduate School, Seoul National University

(Directed by Professor **Won-Jin Yi, PhD**)

Contents

I. Introduction

As implant surgeries have increased because of increasing indications for edentulous patients, surgical complications are also increasing, because of limitations in an operator's experience as well as anatomical variations in patients [1, 2]. Damage to the inferior alveolar nerve or perforation of the maxillary sinus is a common complication of implant surgery [3]. An implant has to be placed in a planned position, angle, and depth exactly in order to reduce complications and increase the long-term success of an implant-supported prosthesis [4, 5]. Conventional computed tomography (CT) can provide 3-dimensional (3D) anatomical information for precise implant planning. However, it is not commonly used because of the its associated cost, radiation risk, and space requirement. Recently, because of its low installation cost, small space requirement, and lower radiation risk, cone-beam computed tomography (CBCT) has been widely used in local dental clinics in order to obtain 3D anatomical images of the jaw [6, 7]. It helps dentists to transfer the implant surgical plan to the patient's jaw bone more exactly by understanding 3D anatomical structures more accurately. Nonetheless, dentists require more experience in order to place an implant exactly in a planned location without surgical complications [8]. Therefore, various methods have been developed in order to perform a proper implant placement at the planned site.

One method involves using a drill guide stent. In this method, accurate positioning of an implant is determined using an implant-planning program with 3D computed tomography (CT) images [9]. Unlike in the conventional method where the stent is made by laboratory work using resin, this stent is made by rapid prototyping [10, 11]. Examples include Nobelgide (Nobel Biocare, Göteborg,

Sweden), SurgiGuide (Materialise Dental, Leuven, Belgium), and Anatomage Guide (Anatomage, San Jose, CA). However, this stent method has some drawbacks, as it requires a considerable amount of time and cost for stent fabrication alone, moreover, intraoperative changes to the preoperative plan are impossible, so a fatal error may occur if the stent is not firmly fixed [12, 13]. Further, surgical access with stent is limited when the patients have limited interocclusal distance because a surgeon has to use a longer drill than usual case due to the thickness of a drill sleeve [14].

Another method for implantation in a precise location is an image guided navigation method. In this method, a position tracking camera is used so the location of the drill can be seen being overlapped on the patient's 3D CT images, and this provides a relative location of the drill in real time on the patient's anatomical structure [15,16,17]. Therefore, an operator can place an implant in a precise position by ensuring the location of the drill tip, angle, and depth while keeping an eye on the planned location for insertion on 3D CT image. Examples of this method include IGI DenX (Denx Ltd., Jerusalem, Israel) and RoboDent (RoboDent GmbH, Berlin, Germany). Its disadvantages include the necessity to fabricate a template in a laboratory, as to use this method, a registration template should be fabricated before surgery, thus requiring at least one-half day of preparation work additionally. Further, surgical preparation is time consuming because of the set up of the navigation devices, and the system costs are expensive. For these reasons, this method is not as widely used as the guide stent method [18, 19]. Therefore, it is necessary to develop a new implant surgery system in order to overcome the drawbacks of the previously mentioned methods.

In this study, in order to simplify surgical preparation, shorten the overall duration of surgery, and minimize inconvenience to the surgeon during surgery, a new image guided navigation system using cone-beam CT was developed for dental implant surgery. The new system uses 3D image for a precise implant surgery, and it could accurately reproduce the planned insertion location, angle, and depth during surgery. Some drawbacks of the conventional image guided navigation surgery system were overcome, and it has made it possible to perform a dental implant surgery all in one visit using the newly developed image guided navigation system.

II. Literature Review

1. Implant surgery using drill guide stent method

Presently, the most actively studied field in precise implant placement is the drill guide stent method. Becker et al. described a procedure for fabricating a precise surgical stent that ensures appropriate implant placement. They reported that despite the time-consuming nature of the stent fabrication procedure, it was worth the effort to ensure long-term success of implants [5]. Sarment et al. compared the accuracy of a conventional surgical stent to that of a stereolithographic surgical stent, and reported that the average distance between the planned implant and the actual osteotomy was 1.5 mm at the entrance and 2.1mm at the apex when the conventional surgical stent was used, and 0.9 mm and 1.0 mm, respectively, when the stereolithographic surgical stent was used. They concluded that implant placement was improved by using a stereolithographic surgical stent [10]. Almeida et al. reviewed 34 studies and reported that the image guided surgery is essential for implants placement, regardless of the surgical technique; however, mistakes may occur during the diagnostic and therapeutic steps [12]. Giacomo et al. placed 60 implants and 12 prostheses in 12 patients to evaluate the accuracy and complications resulting from selective laser sintering surgical stent for flapless dental implant placement. The mean SD angular, coronal, and apical deviations were 6.53 ± 4.31 °, 1.35 ± 0.65 mm, and 1.79 ± 1.01 mm, respectively. The total complication rate was 34.41 %. They concluded that the surgical stent for implant surgery still requires improvements and should be considered in the developmental stage [13]. A review by Jung et al. reported that that the following parameters were

selected to assess implant system accuracy in most studies: A) deviation error in a horizontal direction at the entry point of the drill or implant; B) deviation error in a horizontal direction at the apex of the drill or implant; C) deviations in height; and D) deviations of the axis. They concluded that in systems using surgical stents, the mean error was 1.12 mm at the entry point, 1.2 mm at the apex, and 4.0 ° in angulation [18].

2. Implant surgery using image guided navigation method

1) Image guided navigation

Researches on image guided navigation method have been reported. Sieûegger et al. placed a total of 18 dental implants in 5 patients with aid of image guided navigation to compare the accuracy of conventional and computer-assisted dental implantation planning and surgery. They concluded that the use of an image-guided navigation system provides a valuable tool in implant dentistry and proved superior to conventional implant surgery especially in difficult anatomical regions [17]. Wittwer et al. assessed whether navigated flapless transmucosal implant bed preparation allows placement of dental implants in edentulous mandibles; they reported that navigated flapless transmucosal implant placement was a precise, predictable, and safe procedure in edentulous mandibles [20]. Casap et al. placed 8 implants in a completely edentulous mandible using image guided navigation and reported that the navigation system provided real-time imaging of the drill and transformed flapless implant surgery into a fully monitored procedure [21].

2) Accuracy of image guided navigation

Some studies investigating the accuracy of image guided navigation method have been published. Chui et al. drilled a specially designed acrylic model that simulated a mandible by using IGI DenX and measured the error from the starting point to the planned and drilled holes, angular deviation, and depth error. The mean error of the starting point was 0.43 mm (± 0.56 mm) and the mean angular deviation was 4.0° (± 3.5 °) [22]. Elian et al. placed 14 implants in 6 patients by using IGI DenX; they found that the mean error was 0.89 ± 0.53 mm at the implant head and 0.96 ± 0.50 mm at the apex, while the angular deviation was 3.78 ± 2.76 ° [23]. Ruppin et al. placed 120 implants in 20 human mandibles using navigation systems and stereolithographic stent systems. They found that the error of the starting point, depth error, and angular deviation were 1.1 ± 0.5 mm, 0.6 ± 0.3 mm, and 8.1 ± 4.6 °, respectively, using RoboDent; 1.5 ± 0.8 mm, 0.6 ± 0.4 mm, and 7.9 ± 5 °, respectively, using SimPlant (Materialise Dental, Leuven, Belgium); and did not observe significant differences ($P > 0.05$) [24].

3) Errors in image guided navigation

Widmann et al. reviewed articles about different types of errors in image-guided surgery. In image-guided surgery, total errors are affected by the tracking camera, imaging modality, registration, surgical application, and human errors. They concluded that knowledge of different errors and their contributions to the overall accuracy of image-guided surgery are important and should help the surgeon in the appropriate selection of imaging modality, registration methods, and image guided surgical approaches [25]. Marmulla et al. reported that the geometric mean deviation of NewTom 9000-based CBCT was 0.13 ± 0.09 mm and the CBCT images are suitable for 3-dimensional implant planning [26]. Eggers et al.

compared the geometric accuracy of CBCT to that of conventional CT to assess its suitability for image-guided navigation. The geometric deviation of MDCT and CBCT were 0.17 ± 0.09 mm and 0.37 ± 0.19 mm, respectively. They concluded that the spatial accuracy of CBCT was slightly lower than that of MDCT, but sufficient for image guided navigation. Additionally, accuracy was better in the middle, but lower in the margins of the volume [27]. Kozak et al. developed a new marker for improved registration. They reported that when extracting the center of marker from the image during the registration procedure, a round form was more accurate than an irregular form, and it was more accurate to form a central pivot on marker to physically point the center of marker accurately [28]. Birkfellnet et al. reported that the accuracy of the image guided surgery system was not greatly increased, even if the number of fiducials was increased from 3 to 5 [29]. According to a study by Widmann et al., no significant change in TRE value occurred even if the number of markers increased from 5 to 7 [30]. Abbashi et al. reported that 4 or 8 markers were more accurate than 6 markers [31]. Widmann et al. compared bone markers, a registration template, and an external registration frame which were used for an optical-based navigation system registration, and conclude that the accuracies of the three methods were similar [32]. With regard to handpiece error, Wanschitz et al. observed that the horizontal movement of the handpiece ball bearing was 0.3 mm at the tip while evaluating the accuracy of an image-guided surgical navigation system for mandibular implant placement [33].

III. Materials and Methods

1. Development of a new image guided navigation system for dental implant

1) Procedure of new image guided navigation surgery

The overall procedures of the system are as follows (Fig. 1).

① The registration body was fixed to the patient model by using an improvised bite splint.

② The 3D image of the model wearing the splint was obtained using a CBCT.

③ The preoperative implant planning of position, angle and depth was done.

④ The registration using pre-recorded fiducial positions on the registration body was preceded independently before surgery.

⑤ New offsets of the various drills used during surgery were directly calibrated.

⑥ The location of the drill tip was tracked in real time and it was visualized on a monitor during surgery.

⑦ Implants placed on the planned sites by using the image guided navigation.

2) New tracking tools and improvised patient splint

In the newly developed image guided navigation system, new instrument tracking tool and patient tracking tool were developed. The instrument tracking tool was tightly installed on a handpiece by using a ring-shaped fixation device (Fig. 2A, B and C), which could be applied to any kind of handpieces. As the patient tracking tool could be adjusted to orientate in any direction for free line-of-

sight of the camera with some modifications, it provided universal orientation for maxillary and mandible surgeries (Fig. 3A, B and C).

A registration body was fabricated in order to facilitate registration between the patient and the image spaces. It was an arched frame composed of clear orthodontic self-curing acrylic resin (Ortho-Jet; Lang Dental Manufacturing Co., Wheeling, IL) with 8 ceramic spheres (1 mm diameter) fixed in holes at anterior and bilateral molar sites (Fig. 4A). It was fixed to the patient almost adjacent to the occlusal plane and near the surgical site by using a patient-specific splint. A patient-specific splint was improvised by using a bite splint shortly before the CT scanning without additional laboratory work for fabrication (Fig. 4B). A patient's dental occlusion was recorded on a devised splint by using dental impression material (thixotropic vinyl polysiloxane, Parkell Inc., Edgewood, NY, USA).

3) Development of registration method using a reusable registration body and pre-recorded fiducials

The registration was performed in order to match the phantom's physical space to that of the image space by using a reusable registration body. The method based on the registration body was successfully used for mandibular movement tracking and simulation in our previous studies [34-36]. The registration body and the patient tracking tool were attached to a splint by using a LEGO block (LEGO Danmark A/S, Billund, Denmark) (Fig. 4C). The locations of the spheres on the registration body were registered by using point-to-point matching in sequential order with those identified on the 3D CT image (Fig. 5). The fiducial spheres of the registration body were distributed on the occlusal level and in the dentition curve. Because registration could be performed using the coordinate system of a splint

with the patient tracking tool, it preceded independently before the splint was attached to the patient for surgery. Additionally, the positions of the matched points on the 3D CT image could be recorded and saved for registration in advance. Because a LEGO block was used for attaching the registration body and the patient tracking tool to the splint, the locations of the spheres on the registration body relative to the patient tracking tool were constant. Thus, the location of the spheres relative to the reference could be saved and reused without pointing the physical locations of the spheres in another surgery. These steps played an important role in reducing the operative time. After registration, the registration body could be removed from the splint because it was not necessary for subsequent tracking.

4) Intraoperative tracking and visualization of drill tip position

The instrument tracking tool was tightly installed on a handpiece and the patient tracking tool was attached to the splint. Then, 3D motions of patient and instrument tracking tools were tracked by using an optical camera system (Polaris Vicar, Northern Digital Inc., Ontario, Canada). Continuous image position of the drill was calculated with respect to the patient by applying the Eq.1 to the measured physical positions by the camera. The location of the drill tip was tracked in a 3D image regardless of patient's movement in real time and it was visualized on a monitor during surgery.

$$\boldsymbol{P}_{image} = \boldsymbol{M}_{reg}\boldsymbol{M}_{pat}^{-1}\boldsymbol{M}_{tool}\boldsymbol{P}_{offset} \quad (1)$$

P_{image}: 3D position vector of drill tip in image space,

M_{reg}: Transformation matrix from physical to image spaces,

M_{pat}: Matrix of translation and rotation for patient tracking tool in physical space,

M_{tool}: Matrix of translation and rotation for instrument tracking tool in physical space,

P_{offset}: 3D offset vector from instrument tracking tool to drill tip

5) Direct drill offset determination

During an implant surgery procedure, the drills were exchanged several times in order to form an appropriate hole for each implant. The drilling procedure varied from commercialized implants manufactured by various companies. If the drill was changed, the offset of its tip from the instrument tracking tool was also changed, so a new offset vector had to be calibrated and reflected to the instrument tracking equation (Eq. 1) to track the position of a drill tip accurately. We developed an easy method to determine the offset vector accurately during surgery. The offset vector of a new drill tip was calculated from a known position of a specified point (Eq. 2). It was determined by touching a point with the drill tip point and by pressing a foot-switch without pivoting the tracked handpiece (Fig.6). This method was also applied to the handpiece on which the instrument tracking tool was installed at the first time.

$$\boldsymbol{P}_{offset\_new} = \boldsymbol{M}^{-1}_{tool\_new}\,\boldsymbol{M}_{pat\_old}\,\boldsymbol{P}_{ref\_point} \qquad (2)$$

P_{offset_new}: Offset vector of a new drill tip,

M_{tool_new}: New matrix of translation and rotation for instrument tracking tool,

M_{pat_old}: Old matrix of translation and rotation for patient tracking tool,

P_{ref_point}: Physical position of known point

2. Evaluation of navigation system for dental implant surgery

1) Accuracy of registration and offset determination

The target registration error (TRE) is measured to quantify the registration error from image-guided navigation methods. TRE is the distance between corresponding points not used in calculating the registration. In order to measure the TRE for the developed system, the model had 10 embedded ceramic spheres as landmarks (Fig. 7). After finishing registration, the physical location of the ceramic spheres was localized by using a tracked pointing tool. Then, the root mean square (RMS) difference between true and tracked positions in the image for 10 landmarks was quantified as a registration error (Fig. 8). The TRE of each sphere was measured 10 times with the tracked pointing tool in order to minimize human error when applying the tool. And, the TRE for the registration method using pre-recorded fiducial positions was also quantified using the same ceramic spheres. After recording the physical fiducial positions on a model previously, the physical positions were registered by point-to-point matching with image positions on another model. The RMS difference was also measured ten times at ten landmarks (Fig. 9). Finally, the TRE for the direct determination of a drill offset was measured by using a drill with unknown offset value. First, the coordinates of the landmark (prefabricated cavity) in the connecting part of the patient tracking tool were obtained by using the tracked pointing tool and the drill offset was automatically calculated from the obtained coordinates. By using this offset, the TRE of each ceramic sphere in a model was measured 10 times (Fig. 10).

2) Accuracy of implant placement by the developed system

(1) Phantom and CBCT scanning

A partially edentulous model (Basic-JCP model, Korea model technology, Seoul, Korea) was used to evaluate the accuracy of the developed image guided navigation system (Fig.11). The model had soft tissue and spongious bone in order to simulate a real jaw. A patient-specific splint was firmly mounted onto the teeth of the model. A registration body was attached to the splint in order to facilitate registration between the patient and the image spaces. A 3D image of the model was obtained by using a CBCT (Implagraphy, VATECH, Seoul, Korea) under the condition of 85 kVp, 3.3 mA, 24 sec scan time and 12 x 9 cm^2 field of view (FOV) with voxel size of 0.2 x 0.2 x 0.2 mm^3.

(2) Implant planning

After obtaining CBCT images, implant surgery planning was performed by using commercialized software (InVivoDental, Anatomage, San Jose, CA) (Fig. 12). We planned a total of 110 implant surgeries including to the following sites in 10 models: the maxillary right central incisor, first premolar, first molar, and second molar, and the maxillary left first premolar, second premolar, and first molar, and the mandibular left canine, and first molar, and the mandibular right first molar, and second molar. The 3D center positions at the platform and apex of the planned implant were transformed to our software coordinate system through a simple calculation.

(3) Implant placement

To simulate the patients in real clinical situations, the model was installed on an experimental manikin (KaVo, Biberach, Germany). The implants (Osstem TS III, Osstem Implant, Seoul, Korea) with a 4.0 mm diameter and 10 mm length were placed in planned sites of each model by using the developed image guided

navigation system (Fig. 13). The drilling sequence for the implant socket was performed following the manufacturer's surgical implant protocol. The preparation of the insertion socket was started with a lance drill in order to mark the primary central position of the implants on the gingiva, and a tissue punch was used in order to remove the gingiva at this location. In the next step, a 2 mm diameter twist drill was used to generate the preliminary implant socket. In order to increase the diameter of the socket, a pilot drill was applied, and a twist drill with a diameter of 3 mm, 3.3 mm, and 4.0 mm cortical drill was used in ascending order (Fig.14). After completion of the socket preparation, the implant was placed by using an unmounted driver. During a flapless procedure, the developed navigation surgery system provided relative real-time locations of the drill in the CBCT images. An experienced clinician who had a total of 10 years' experience performed all the insertions.

(4) Error quantification

After placing the implants, the registration body was attached to the model again and CBCT images were obtained with the same imaging parameters and scanner as the first scanning. The post-operative CBCT image was registered with the pre-operative CBCT image by point-to-point matching of the fiducial positions used in registration (Fig. 15). Then the RMS differences between the planned and placed center points at the platform and apex of the implant, respectively, were quantified as positional deviation (Eq. 3). The angle between the lines connecting the platform center point and the apex of the planned and placed implants was also calculated as angular deviation (Eq. 4) (Fig. 16).

$$E_{rms} = \sqrt{(x_f - x_p)^2 + (y_f - x_p)^2 + (z_f - x_p)^2} \quad (3)$$

(x_f, y_f, z_f) : The center point at the platform and apex of the placed implant,

(x_p, y_p, z_p) : The center point at the platform and apex of the planned implant

$$\theta = \arccos\left(\frac{v_f \cdot v_p}{|v_f||v_p|}\right)$$
$$v_f = (x_{hf} - x_{tf}, y_{hf} - y_{tf}, z_{hf} - z_{tf})$$
$$v_p = (x_{hp} - x_{tp}, y_{hp} - y_{tp}, z_{hp} - z_{tp}) \quad (4)$$

(x_{hf}, y_{hf}, z_{hf}) : The center point at the platform of the placed implant,

(x_{tf}, y_{tf}, z_{tf}) : The center point at the apex of the placed implant,

(x_{hp}, y_{hp}, z_{hp}) : The center point at the platform of the planned implant,

(x_{tp}, y_{tp}, z_{tp}) : The center point at the apex of the planned implant,

v_f : The vector in the direction of the placed implant,

v_p : The vector in the direction of the planned implant

3) Statistical analysis

A one-way analysis of variance (ANOVA) was performed to identify the TRE differences for registrations and the offset determination method and to analyze the differentiability of implant placement accuracy in different models and implant sites. A probability level of 0.05 was regarded as significant.

IV. Results

In this study, image guided navigation system based on an optical tracking camera was developed and CBCT images was used in the developed system. New instrument tracking tool and patient tracking tool were developed. A patient-specific splint was improvised using a bite splint and dental impression material. Registration method using a reusable registration body and pre-recorded fiducials was developed. Also, direct offset determination method was developed.

The implants were placed on the planned sites of each model by using the developed navigation surgery system (Fig. 13). Figure 17 shows the intraoperative screen of the navigation system. The navigation system provides the practitioners with 3-dimensional view of the patient's anatomy. The positional difference between the location of drill tip and planned position of implant was quantified and visualized on the 3D view in real-time.

Table I shows the mean TRE of the registration method using a registration body, registration by pre-recorded fiducials, and direct offset determination in a model. The total mean (± SD) TRE was 0.35 ± 0.11, 0.34 ± 0.18, and 0.35 ± 0.16 mm, respectively. An ANOVA demonstrated no significant difference regarding accuracy among the methods ($P > 0.05$). Figure 15 shows the mean errors and angular deviation between planned and placed implants according to the models and Table II shows these values for each location. The total mean error was 0.41 ± 0.12 mm at the center point of the platform and 0.56 ± 0.14mm at the center point of the apex, and 2.64 ± 1.31° was the angular deviation of the long axis of the implant. Table II also shows the maximum and minimum errors and angular

deviations between planned and placed implants. The maximum error was 0.72 mm at the center point of the platform and 0.98 mm at the center point of the apex, and 6.20 ° was the angular deviation. No significant differences existed in any of the 10 models ($P > 0.05$), and no significant differences existed for any of the 11 teeth or in any site (upper, lower, left, right, and front) ($P > 0.05$).

V. Discussion

Image-guided navigation surgery was first performed for neurosurgeries in the 1980s by using a stereotactic frame [37, 38]. Since then, improvements in hardware such as CT scanners, computers, and location-tracking cameras, and in software have increased the applications of this method. In craniomaxillofacial surgery, this method has been successfully conducted for anatomically complicated field such as tumor removal, temporomandibular joint surgery, and orthognathic surgery [39, 40]. Recently, an image guided navigation method has been used in implant surgery [20-24, 41, 42]. Because this developing technology provides the relative location of the drill in real time on a patient's anatomical structure, a clinician can precisely place implants according to the preoperative plan while avoiding critical anatomic structures [16, 17]. However, this method has not been frequently used for clinical treatment because it requires a lot of time, has the increased costs of surgical preparation, and involves some inconveniences because of the navigational devices that are used [18, 19]. In our newly developed system, the disadvantages of conventional systems were improved, and the accuracy of the developed system was evaluated.

The clinical use of an image guided navigation system largely depends on its accuracy. Implant placement must be highly accurate from a prosthetic and anatomical point of view. Therefore, it is important to analyze the accuracy of an image guided navigation system in order to increase the accuracy of implant placement. Its accuracy had been assessed by various methods both preclinically and clinically in previous studies and defined as the locational and angular deviation of the plan compared to the result [15, 18]. The mean error was reported

to range from 0.35 mm to 0.89 mm at the entry point, 0.6 mm to 0.96 mm at the apex and 0.83 to 8.1 degrees for the angle according to the study designs [43-48]. In vitro studies, Brief et al. compared image guided navigation and manual implant surgeries by preparing a bore hole in a mandibular model. The mean error at the entry point was 1.35 mm in manual implant surgery and 0.35–0.65 mm in image guided navigation implant surgery (RoboDent and IGI DenX). Moreover, the mean error at the end point was 1.89 mm in manual implant surgery and 0.60–0.94 mm in image guided navigation implant surgery; the mean angular deviation was 4.59 ° and 2.12–4.21 °, respectively [49]. In a recent study, Widmann et al. performed 104 drillings on stone casts. The mean total error at the tip of the borehole was 0.88 ± 0.65 mm. The mean lateral errors were 0.51 ± 0.49 mm at the base and 0.46 ± 0.34 mm at the tip of the borehole, respectively. The mean angular error was 0.83 ± 0.60 ° (0.0 to 2.5 °) [50]. Those values were lower than the mean errors reported in the previous studies because an aiming device was used to conduct the drilling. In vivo studies, Wittwer et al. placed 78 implants in 20 patients by using StealthStation Treon (Medtronic, Minneapolis, MN) and reported that the mean error was 0.8 ± 0.6 mm at the implant tip and 1.1 ± 0.7 mm at the coronal end [41]. Furthermore, Jung et al. reviewed 19 articles and concluded that the mean error was 0.62 mm at the entry point, 0.68 mm at the apex, and 4.0 ° in angulation [18]. Actual implant placement cases demonstrated a larger error than that of those in which only a drill hole was formed, and models or cadavers showed smaller error than patients. This finding was related to the fact that the procedure is limited by the presence of blood and saliva or by patient movement [18].

In this study, after placing the implants, post-operative CBCT images were

registered with pre-operative CBCT images in order to evaluate the accuracy of the developed system. The positional deviation between the center points of planned and placed implants at the platform and apex was quantified as a RMS (Eq. 3). The angular deviation error between long axis of planned and placed implants was calculated (Eq. 4). A total of 110 implants in the 11 sites of 10 models were placed in flapless surgery method by using image guided navigation surgery system. The mean error between 110 planned implants and placed implants was 0.41 ± 0.12 mm at the center point of the platform and 0.56 ± 0.14 mm at the center point of the apex and the angular deviation was 2.64.± 1.31°. Therefore, the developed system had slightly improved accuracy compared with that of the results from the Jung et al. study. An ANOVA analysis revealed no significant differences among the models, surgical sites, and arch positions. In a developed navigation system, because the positional differences between the location of the drill tip and the planned implant position were quantified and visualized on the 3D view in real-time, an operator could check the quantified error in real-time during surgery. This enabled the operator to place the implants more accurately.

In addition to the accuracy of the image guided navigation system, it is also important to know the maximum deviation, which is crucial for avoiding injury to essential anatomic structures. Clinicians should know a safe distance that is at least equivalent to the maximum deviation of an individual system. Kramer et al. placed implants in the maxillary central incisor and canine areas of a plaster model and reported that the maximum error was from 0.8 to 1 mm at the entry point whit a conventional implant placement and 0.6 mm with a navigation system and that the maximum angular deviation was from13° with a conventional implant placement

and 7 ° with a navigation system [51]. In this study, the maximum error was 0.72 mm at the platform and 0.98 mm at the apex and the angular deviation was 6.20 °, which were similar to those of the Kramer et al study. Thus, one mm is the recommended safety margin around the anatomical structures in a developed navigation system.

The accuracy of a navigation system is most affected by the accuracy of registration. This is in turn affected by the size, form, material, number, and distribution of the fiducial markers and the manner in which they are fixed in a patient [25, 52-55]. According to Marmulla et al, if a marker was located between two CT slices during imaging, its location could be mismeasured [52]. Therefore, the registration is more accurate if the marker size is larger than the image voxel size and when the voxel size is reduced [53]. In this study, markers of 1 mm that were is larger than the voxel size of 0.2 mm, were used.

In an image guided navigational surgery, there are registration methods of bone marker registration, registration template, and external registration frame according to the marker fixation methods. The bone marker registration is the most accurate method because a change in the marker location does not occur between CT image scanning and registration, but it requires an invasive procedure in order to fix the marker to a bone [30, 41]. The registration template method and external registration frame method are noninvasive. Markers for the external registration frame can be widely distributed compared to those of the registration template method, but its bulky frame requires sufficient fixation so the location does not change [56]. In the registration template method, a relatively small template is firmly fixed to the remaining tooth, but it requires additional time, as well as

laboratory work, in order to fabricate a splint with a patient's cast model [30, 56]. In this study, a patient-specific splint was improvised using a bite splint and dental impression material without additional laboratory work for fabrication. Dental occlusion of the patient recorded on the devised splint that provided the synchronization of the marker positions between CBCT scanning and registration. No laboratory work for fabricating the splint was necessary, and no sterilization as the splint was disposable. We also used a reusable registration body, which could be easily attached to and detached from a patient's splint. The physical fiducial positions on the registration body were previously recorded and could be used for another registration without measuring the fiducial positions again if the position of the patient tracking tool did not change with respect to the world coordinate system between surgeries for different patients. The registration body could be removed from the splint during surgery. This feature saved time, decreased the labor necessary for surgical preparation, and additionally minimized the inconvenience to the surgeon during surgery.

In general, the TRE is measured to quantify registration errors from intraoperative image-guided navigation methods. The TRE is the distance between corresponding points not used during registration. Usually, the TRE increases according to the growing distance between the points that are used for calculating the error and the fiducial marker, which is used for registration [56, 57]. The TRE was reported to range from 0.35 ± 0.14 mm to 2.31 ± 0.38 mm according to the target location, the image modalities and the fixation method of the fiducial markers [32, 55, 57-59]. In this study, the fiducial markers of the registration body were distributed on the occlusal level in the dentition curve, so the physical

landmark location that was used for calculating the TRE was close to the fiducials. As a result, the TRE, 0.35 ± 0.11 mm, of the registration method was high using a registration body, as compared with that of the previous studies, and the TRE, 0.34 ± 0.18 mm, of the method was also high using pre-recorded fiducials and showed no statistical difference. As a result, the registration body method provided high registration accuracy over the whole edentulous dentition in this study.

In this study, an instrument tracking tool was tightly installed on a handpiece by using a ring-shaped fixation device, which could be applied to any kind of handpieces. The patient tracking tool also provided a universal orientational configuration for maxillary and mandibular surgeries as it could be adjusted to orient in the direction for free line-of-sight of the camera with some modifications. During the implant surgery procedure, the drills were exchanged several times to form an appropriate hole for each implant. The drilling procedure varied from commercialized implants manufactured by various companies. When the drill changed during surgery, the offset of the drill tip from the instrument tracking tool was changed, so a new offset vector had to be reflected to the instrument tracking equation to track the drill tip position accurately. An inaccurate offset value during tracking the instrument could result in fatal errors to patients during surgery. In conventional navigation systems, only the drills of which the offset vector was previously known and registered could be used during surgery. The pivoting method used for measuring the offset generally was difficult to be applied directly to the handpiece during surgery because its shape is not that of a straight line from its tip to the tracked marker. Therefore, we developed an easy method for determining the offset vector accurately during surgery. The offset vector of a new

drill tip could be directly determined from a specified point with a known position. The TRE, 0.34 ± 0.16 mm, for the direct determination of a drill offset was high and showed no statistical difference. These new tools and procedures increased the convenience and usability of the developed system.

Recently, CBCT has become a common 3D imaging modality in dental clinics due to its shorter scan time, lower cost, smaller occupation space and lower radiation dose than multislice computed tomography (MSCT) [6, 7, 60]. The mean TRE was 1.50 ± 0.82 mm with CBCT and 1.57 ± 0.84 mm with MSCT image data and they did not differ significantly after pair-point registration [61]. After measurements of distances between markers were obtained using an image guided navigation system, the mean errors were 0.43 mm for MSCT and 0.46 mm for CBCT, and showed no statistically significant difference [62]. Therefore, CBCT demonstrated an equivalent accuracy to that of MSCT for an image-guided navigation implant surgery. In this study, the CBCT images of the models were obtained before and after implant placement. The mean error between the planned and installed implants was 0.41 ± 0.12 mm at the platform and 0.56 ± 0.14 mm at the apex, and showed higher accuracy compared with those of the previous studies using MSCT [22, 49-51].

Ewers et al. reported that image-guided navigation implant surgery initially required 2–3 days but could be completed in half a day because of software optimization for dental implants since the end of 2000 [16]. In our developed navigation system, the surgical preparation procedure was simplified because of the use of a bite splint and dental impression material without additional laboratory work for fabrication, and CBCT images. The surgical preparation procedure was

shorter in duration than Ewers et al. Therefore, these factors made it possible to perform a dental implant surgery based on the navigational guidance in all-in-one visit. However, in this study, only one clinician who had a total of 10 year experience placed the implants, and the experiment was performed under controlled conditions. Thus, operator's experience as well as the in vitro nature of this study might influence the total error.

Moreover, we plan to further study our navigation system by using a completely automatic registration in which the center point of a marker on a CBCT image would be automatically extracted. A navigation control would also be utilized in order to increase safety by allowing for an automatic turn off in case any deviation from the planned area occurred during surgery. Furthermore, any discomfort associated with viewing the operative site and monitor simultaneously during surgery would be reduced by applying a head-mounted display, so an operator could better focus on the surgery.

In conclusion, a new CBCT image-based method for dental implant navigation surgery was developed to overcome some of the disadvantages with the conventional method, and the accuracy of our system was sufficiently high for clinical application. It would be possible to perform a dental implant surgery in all-in-one visit by using the developed navigational image guidance based on CBCT images. In future studies, both experienced and inexperienced clinicians should assess the accuracy of the developed navigation system in clinical situations.

VI. References

1. Zoghbi SA, de Lima LA, Saraiva L, Romito GA. Surgical experience influences 2-stage implant osseointegration. J Oral Maxillofac Surg 2011; 69: 2771-6.
2. Chee W, Jivraj S. Failures in implant dentistry. Br Dent J 2007; 202: 123-9.
3. Greenstein G, Cavallaro J, Romanos G, Tarnow D. Clinical recommendations for avoiding and managing surgical complications associated with implant dentistry: a review. J Periodontol 2008; 79: 1317-29.
4. Buser D, Martin W, Belser UC. Optimizing esthetics for implant restorations in the anterior maxilla: anatomic and surgical considerations. Int J Oral Maxillofac Implants 2004; 19 Suppl: 43-61.
5. Becker CM, Kaiser DA. Surgical guide for dental implant placement. J Prosthet Dent 2000; 83: 248-51.
6. Benavides E, Rios HF, Ganz SD, An CH, Resnik R, Reardon GT, et al. Use of cone beam computed tomography in implant dentistry: the International Congress of Oral Implantologists consensus report. Implant Dent 2012; 21: 78-86.
7. Quereshy FA, Savell TA, Palomo JM. Applications of cone beam computed tomography in the practice of oral and maxillofacial surgery. J Oral Maxillofac Surg 2008; 66: 791-6.
8. Van de Velde T, Glor F, De Bruyn H. A model study on flapless implant placement by clinicians with a different experience level in implant surgery. Clin Oral Implants Res 2008; 19: 66-72.

9. Huh YJ, Choi BR, Huh KH, Yi WJ, Heo MS, Lee SS, Choi SC. In-vitro study on the accuracy of a simple-design CT-guided stent for dental implants. Imaging Sci Dent. 2012; 42: 139-46.

10. Sarment DP, Sukovic P, Clinthorne N. Accuracy of implant placement with a stereolithographic surgical guide. Int J Oral Maxillofac Implants 2003; 18: 571-7.

11. Soares MM, Harari ND, Cardoso ES, Manso MC, Conz MB, Vidigal GM Jr. An in vitro model to evaluate the accuracy of guided surgery systems. Int J Oral Maxillofac Implants 2012; 27: 824-31.

12. de Almeida EO, Pellizzer EP, Goiatto MC, Margonar R, Rocha EP, Freitas AC Jr, et al. Computer-guided surgery in implantology: review of basic concepts. J Craniofac Surg 2010; 2: 1917-21.

13. Di Giacomo GA, da Silva JV, da Silva AM, Paschoal GH, Cury PR, Szarf G. Accuracy and complications of computer-designed selective laser sintering surgical guides for flapless dental implant placement and immediate definitive prosthesis installation. J Periodontol 2012; 83: 410-9.

14. Park C, Raigrodski AJ, Rosen J, Spiekerman C, London RM. Accuracy of implant placement using precision surgical guides with varying occlusogingival heights: an in vitro study. J Prosthet Dent. 2009; 101: 372-81.

15. Widmann G, Bale RJ. Accuracy in computer-aided implant surgery - areview. Int J Oral Maxillofac Implants 2006; 21: 305-13.

16. Ewers R, Schicho K, Truppe M, Seemann R, Reichwein A, Figl M, et al.

Computer-aided navigation in dental implantology: 7 years of clinical experience. J Oral Maxillofac Surg 2004; 62: 329-34.

17. Sieûegger M, Schneider BT, Mischkowski RA, Lazar F, Krug B, Klesper B, et al. Use of an image-guided navigation system in dental implant surgery in anatomically complex operation sites. J Craniomaxillofac Surg 2001; 29: 276-81.
18. Jung RE, Schneider D, Ganeles J, Wismeijer D, Zwahlen M, Hämmerle CH, et al. Computer technology applications in surgical implant dentistry: a systematic review. Int J Oral Maxillofac Implants 2009; 24: 92-109.
19. Mischkowski RA, Zinser MJ, Neugebauer J, Kübler AC, Zöller JE. Comparison of static and dynamic computer-assisted guidance methods in implantology. Int J Comput Dent 2006; 9: 23-35.
20. Wittwer G, Adeyemo WL, Schicho K, Figl M, Enislidis G. Navigated flapless transmucosal implant placement in the mandible: a pilot study in 20 patients. Int J Oral Maxillofac Implants 2007; 22: 801-7.
21. Casap N, Tarazi E, Wexler A, Sonnenfeld U, Lustmann J. Intraoperative computerized navigation for flapless implant surgery and immediate loading in the edentulous mandible. Int J Oral Maxillofac Implants 2005; 20: 92-8.
22. Chiu WK, Luk WK, Cheung LK. Three-dimensional accuracy of implant placement in a computer-assisted navigation system. Int J Oral Maxillofac Implants 2006; 21: 465-70.
23. Elian N, Jalbout ZN, Classi AJ, Wexler A, Sarment D, Tarnow DP. Precision of flapless implant placement using real-time surgical navigation: a case series.

Int J Oral Maxillofac Implants2008; 23: 1123-7.

24. Ruppin J, Popovic A, Strauss M, Spüntrup E, Steiner A, Stoll C. Evaluation of the accuracy of three different computer-aided surgery systems in dental implantology: optical tracking vs. stereolithographic splint systems. Clin Oral Implants Res. 2008; 19: 709-16.
25. Widmann G, Stoffner R, Bale R. Errors and error management in image-guided craniomaxillofacial surgery. Oral Surg Oral Med Oral Pathol Oral Radiol Endod 2009; 107: 701-15.
26. Marmulla R, Wörtche R, Mühling J, Hassfeld S. Geometric accuracy of the NewTom 9000 Cone Beam CT. Dentomaxillofac Radiol. 2005; 34: 28-31.
27. Eggers G, Klein J, Welzel T, Mühling J. Geometric accuracy of digital volume tomography and conventional computed tomography. Br J Oral Maxillofac Surg. 2008; 46: 639-44.
28. Kozak J, Nesper M, Fischer M, Lutze T, Göggelmann A, Hassfeld S, Wetter T. Semiautomated registration using new markers for assessing the accuracy of a navigation system. Comput Aided Surg. 2002; 7: 11-24.
29. Birkfellner W, Solar P, Gahleitner A, Huber K, Kainberger F, Kettenbach J, Homolka P, Diemling M, Watzek G, Bergmann H. In-vitro assessment of a registration protocol for image guided implant dentistry. Clin Oral Implants Res. 2001; 12: 69-78.
30. Widmann G, Stoffner R, Schullian P, Widmann R, Keiler M, Zangerl A, et al. Comparison of the accuracy of invasive and noninvasive registration methods for image-guided oral implant surgery. Int J Oral Maxillofac Implants 2010; 25:

491-8.

31. Abbasi HR, Hariri S, Martin D, Shahidi R. A comparative statistical analysis of neuronavigation systems in a clinical setting. Stud Health Technol Inform. 2001; 81: 11-7.
32. Widmann G, Zangerl A, Schullian P, Fasser M, Puelacher W, Bale R. Do image modality and registration method influence the accuracy of craniofacial navigation? J Oral Maxillofac Surg 2012; 70: 2165-73.
33. Wanschitz F, Birkfellner W, Watzinger F, Schopper C, Patruta S, Kainberger F, Figl M, Kettenbach J, Bergmann H, Ewers R. Evaluation of accuracy of computer-aided intraoperative positioning of endosseous oral implants in the edentulous mandible. Clin Oral Implants Res. 2002; 13 : 59-64
34. Kim DS, Choi SC, Lee SS, Heo MS, Huh KH, Hwang SJ, Yi WJ. Correlation between 3-dimensional facial morphology and mandibular movement during maximum mouth opening and closing. Oral Surg Oral Med Oral Pathol Oral Radiol Endod. 2010; 10: 648-56.
35. Kim SG, Kim DS, Choi SC, Lee SS, Heo MS, Huh KH, Hwang SJ, Yi WJ. The relationship between three-dimensional principal rotations and mandibular deviation. Oral Surg Oral Med Oral Pathol Oral Radiol Endod. 2010; 110: e52-60.
36. Kim SH, Kim DS, Huh KH, Lee SS, Heo MS, Choi SC, Hwang SJ, Yi WJ. Direct and continuous localization of anatomical landmarks for image-guided orthognathic surgery. Oral Surg Oral Med Oral Pathol Oral Radiol. 2013; 116: 402-10.
37. Kelly PJ, Alker GJ Jr, Goerss S. Computer-assisted stereotactic microsurgery

for the treatment of intracranial neoplasms. Neurosurgery 1982; 10: 324-31.

38. Kelly PJ, Kall B, Goerss S, Alker GJ Jr. Precision resection of intra-axial CNS lesions by CT-based stereotactic craniotomy and computer monitored CO2 laser. Acta Neurochir (Wien) 1983; 68: 1-9.
39. Ewers R, Schicho K, Undt G, Wanschitz F, Truppe M, Seemann R, et al. Basic research and 12 years of clinical experience in computer-assisted navigation technology: a review. Int J Oral Maxillofac Surg 2005; 34: 1-8.
40. Wagner A, Undt G, Watzinger F, Wanschitz F, Schicho K, Yerit K, et al. Principles of computer-assisted arthroscopy of the temporomandibular joint with optoelectronic tracking technology. Oral Surg Oral Med Oral Pathol Oral Radiol Endod 2001; 92: 30-7.
41. Wittwer G, Adeyemo WL, Schicho K, Gigovic N, Turhani D, Enislidis G. Computer-guided flapless transmucosal implant placement in the mandible: a new combination of two innovative techniques. Oral Surg Oral Med Oral Pathol Oral Radiol Endod 2006; 101: 718-23.
42. Casap N, Kreiner B, Wexler A, Kohavi D. Flapless approach for removal of bone graft fixing screws and placement of dental implants using computerized navigation: a technique and case report. Int J Oral Maxillofac Implants 2006; 21: 314-9.
43. Wanschitz F, Birkfellner W, Watzinger F, Schopper C, Patruta S, Kainberger F, et al. Evaluation of accuracy of computer-aidedintraoperative positioning of endosseous oral implants in the edentulous mandible. Clin Oral Implants Res 2002; 13: 59-64.
44. Gaggl A, Schultes G, Kärcher H. Navigational precision of drilling tools

preventing damage to the mandibular canal. J Craniomaxillofac Surg 2001; 29: 271-5.

45. Gaggl A, Schultes G. Assessment of accuracy of navigated implant placement in the maxilla. Int J Oral Maxillofac Implants 2002; 17: 263-70.
46. Widmann G, Widmann R, Widmann E, Jaschke W, Bale R. Use of a surgical navigation system for CT-guided template production. Int J Oral Maxillofac Implants 2007; 22: 72-8.
47. Widmann G, Widmann R, Widmann E, Jaschke W, Bale RJ. In vitro accuracy of a novel registration and targeting technique for image-guided template production. Clin Oral Implants Res 2005; 16: 502-8.
48. Hoffmann J, Westendorff C, Gomez-Roman G, Reinert S. Accuracy of navigation-guided socket drilling before implant installation compared to the conventional free-hand method in a synthetic edentulous lower jaw model. Clin Oral Implants Res 2005; 16: 609-14.
49. Brief J, Edinger D, Hassfeld S, Eggers G. Accuracy of image-guided implantology. Clin Oral Implants Res 2005; 16: 495-501.
50. Widmann G, Keiler M, Zangerl A, Stoffner R, Longato S, Bale R, et al. Computer-assisted surgery in the edentulous jaw based on 3 fixed intraoral reference points. J Oral Maxillofac Surg 2010; 68: 1140-7.
51. Kramer FJ, Baethge C, Swennen G, Rosahl S. Navigated vs. conventional implant insertion for maxillary single tooth replacement: a comparative in vitro study. Clin Oral Implants Res 2005; 16: 60-8.
52. Marmulla R, Hassfeld S, Luth T, Muhling J. Laser-scan-based navigation in cranio-maxillofacial surgery. J Craniomaxillofac Surg 2003; 31: 267-77.

53. Maurer CR Jr, Fitzpatrick JM, Wang MY, Galloway RL Jr, Maciunas RJ, Allen GS. Registration of head volume images using implantable fiducial markers. IEEE Trans Med Imaging 1997; 16: 447-62.

54. Abbasi HR, Hariri S, Martin D, Shahidi R. A comparative statistical analysis of neuronavigation systems in a clinical setting. Stud Health Technol Inform 2001; 81: 11-17.

55. Birkfellner W, Solar P, Gahleitner A, Huber K, Kainberger F, Kettenbach J, et al. In-vitro assessment of a registration protocol for image guided implant dentistry. Clin Oral Implants Res 2001; 12: 69-78.

56. West JB, Fitzpatrick JM, Toms SA, Maurer CR Jr, Maciunas RJ. Fiducial point placement and the accuracy of point-based, rigid body registration. Neurosurgery 2001; 48: 810-7.

57. Casap N, Wexler A, Persky N, Schneider A, Lustmann J. Navigation surgery for dental implants: assessment of accuracy of the image guided implantology system. J Oral Maxillofac Surg 2004; 62: 116-9.

58. Eggers G, Mühling J, Marmulla R. Template-based registration for image-guided maxillofacial surgery. J Oral Maxillofac Surg. 2005; 63: 1330-6.

59. Labadie RF, Shah RJ, Harris SS, Cetinkaya E, Haynes DS, Fenlon MR, et al. In vitro assessment of image-guided otologic surgery: submillimeter accuracy within the region of the temporal bone. Otolaryngol Head Neck Surg 2005; 132: 435-42.

60. Loubele M, Bogaerts R, Van Dijck E, Pauwels R, Vanheusden S, Suetens P, et al. Comparison between effective radiation dose of CBCT and MSCT scanners for dentomaxillofacial applications. Eur J Radiol 2009; 71: 461-8.

61. Eggers G, Senoo H, Kane G, Mühling J. The accuracy of image guided surgery based on cone beam computer tomography image data. Oral Surg Oral Med Oral Pathol Oral Radiol Endod 2009; 107: e41-8.

62. Poeschl PW, Schmidt N, Guevara-Rojas G, Seemann R, Ewers R, Zipko HT, et al. Comparison of cone-beam and conventional multislice computed tomography for image-guided dental implant planning. Clin Oral Investig 2013; 17: 317-24.

Tables

Table I. Mean target registration errors for the registration method by using a registration body, for registration by pre-recorded fiducials, and for direct determination of drill offsets at the 10 landmarks (± SD).

Landmark	Registration using registration body (mm)	Registration using pre-recorded fiducials (mm)	Direct drill offset (mm)
1	0.45 ± 0.06	0.36 ± 0.12	0.38 ± 0.06
2	0.31 ± 0.07	0.37 ± 0.12	0.26 ± 0.16
3	0.30 ± 0.08	0.18 ± 0.07	0.41 ± 0.15
4	0.42 ± 0.05	0.66 ± 0.17	0.45 ± 0.07
5	0.29 ± 0.08	0.24 ± 0.08	0.26 ± 0.05
6	0.33 ± 0.13	0.31 ± 0.12	0.48 ± 0.18
7	0.39 ± 0.12	0.46 ± 0.17	0.46 ± 0.22
8	0.30 ± 0.06	0.25 ± 0.13	0.28 ± 0.13
9	0.26 ± 0.06	0.27 ± 0.08	0.35 ± 0.11
10	0.44 ± 0.12	0.34 ± 0.11	0.19 ± 0.04
Total	0.35 ± 0.11	0.34 ± 0.18	0.35 ± 0.16

Table II. Mean, maximum (Max) and minimum (Min) positional deviations between planned and placed implants, and angular deviations for locations (± SD).

Tooth position	Platform (mm)			Apex (mm)			Angle (degrees)		
	Mean ± SD	Max	Min	Mean ± SD	Max	Min	Mean ± SD	Max	Min
Maxillary right central incisors	0.40 ± 0.10	0.49	0.20	0.54 ± 0.11	0.28	0.69	3.23 ± 1.18	5.69	2.22
Maxillary right first premolar	0.36 ± 0.13	0.60	0.20	0.57 ± 0.08	0.66	0.45	2.77 ± 1.20	4.98	1.15
Maxillary right first molar	0.42 ± 0.09	0.60	0.20	0.59 ± 0.18	0.85	0.20	1.85 ± 0.88	3.46	1.12
Maxillary right second molar	0.39 ± 0.12	0.63	0.20	0.60 ± 0.21	0.98	0.28	2.92 ± 1.46	6.20	1.04
Maxillary left first premolar	0.41 ± 0.14	0.66	0.20	0.52 ± 0.08	0.72	0.45	2.69 ± 1.06	4.73	1.17
Maxillary left second premolar	0.47 ± 0.12	0.66	0.20	0.58 ± 0.12	0.82	0.40	2.48 ± 1.56	6.03	0.19
Maxillary left first molar	0.45 ± 0.15	0.72	0.28	0.60 ± 0.14	0.85	0.45	2.84 ± 1.13	4.73	0.48
Mandibular left canine	0.42 ± 0.10	0.63	0.20	0.56 ± 0.17	0.98	0.28	2.93 ± 1.31	5.75	1.13
Mandibular left first molar	0.38 ± 0.09	0.49	0.20	0.52 ± 0.13	0.63	0.20	2.71 ± 1.47	5.84	1.10
Mandibular right first molar	0.33 ± 0.10	0.45	0.20	0.46 ± 0.14	0.66	0.28	2.05 ± 1.24	4.90	0.03
Mandibular right second molar	0.43 ± 0.09	0.63	0.28	0.59 ± 0.10	0.80	0.40	2.54 ± 1.13	4.70	1.14
Total mean	0.41 ± 0.12	0.72	0.20	0.56 ± 0.14	0.98	0.20	2.64 ± 1.31	6.20	0.03

Figures

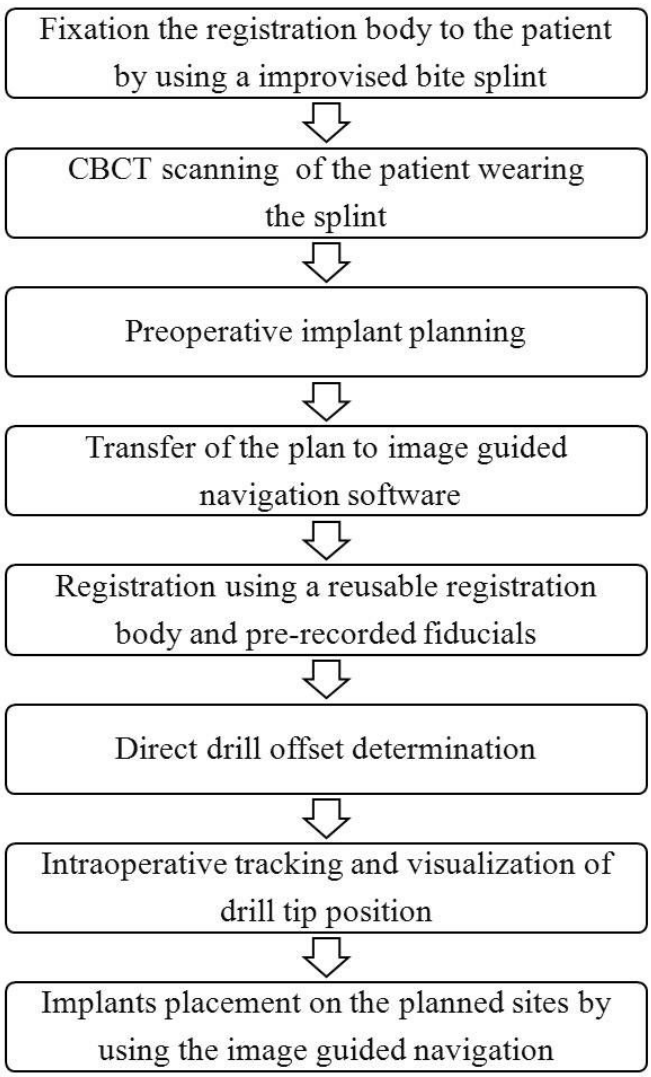

Fig. 1. The overall procedures of the developed image-guided navigation method.

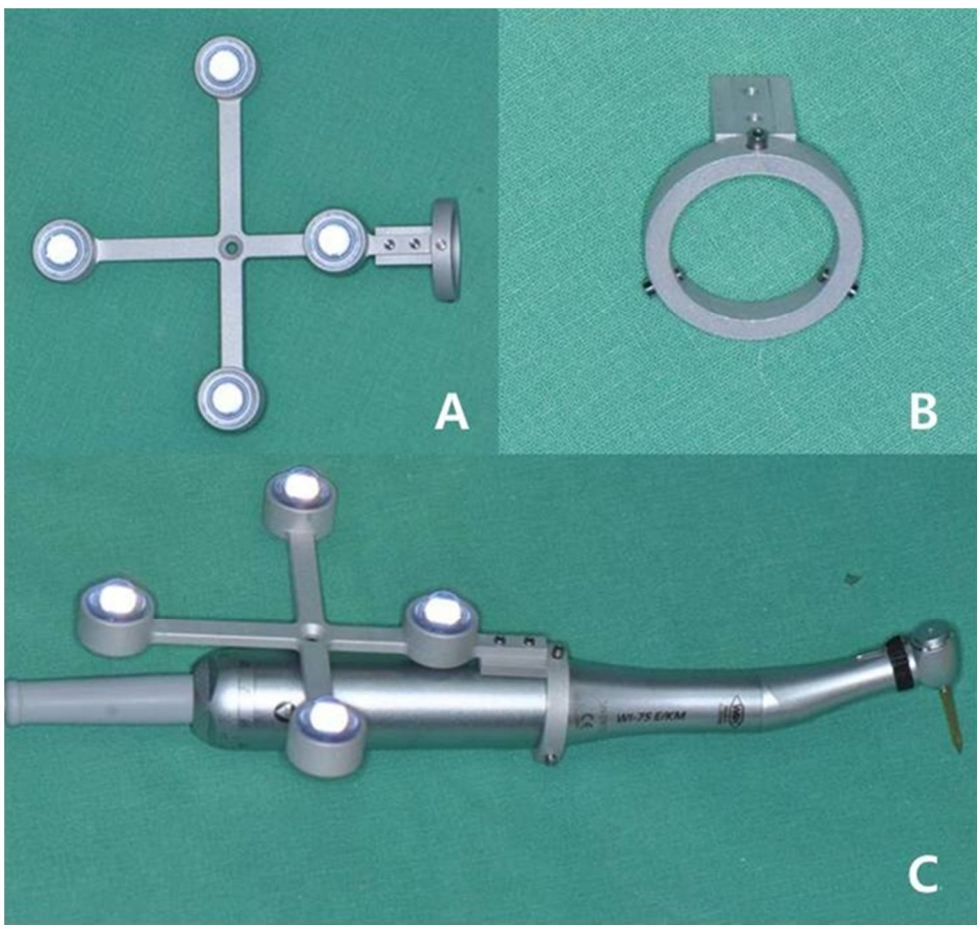

Fig. 2. A. An instrument tracking tool. B. A ring-shaped fixation device. C. The instrument tracking tool is tightly installed on a handpiece by using a ring-shaped fixation device.

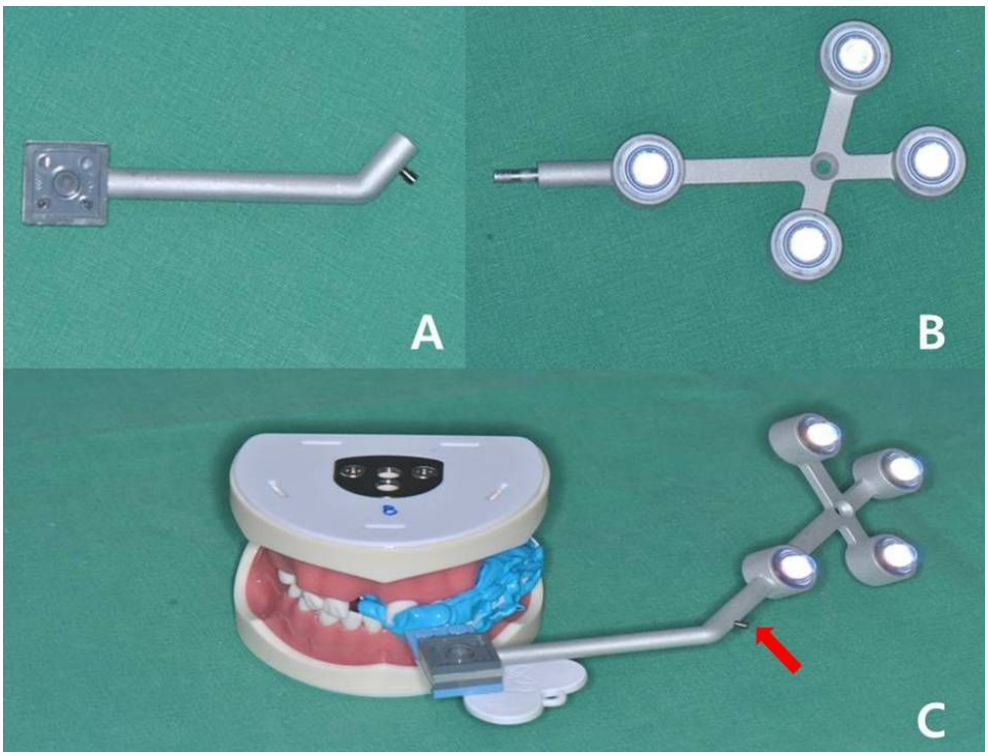

Fig. 3. A. A device fixing patient tracking tool. B. A rotational patient tracking tool. C. The patient tracking tool can be adjusted to orientate in any direction for free line-of-sight of the camera with some modifications. The arrow indicates rotational part.

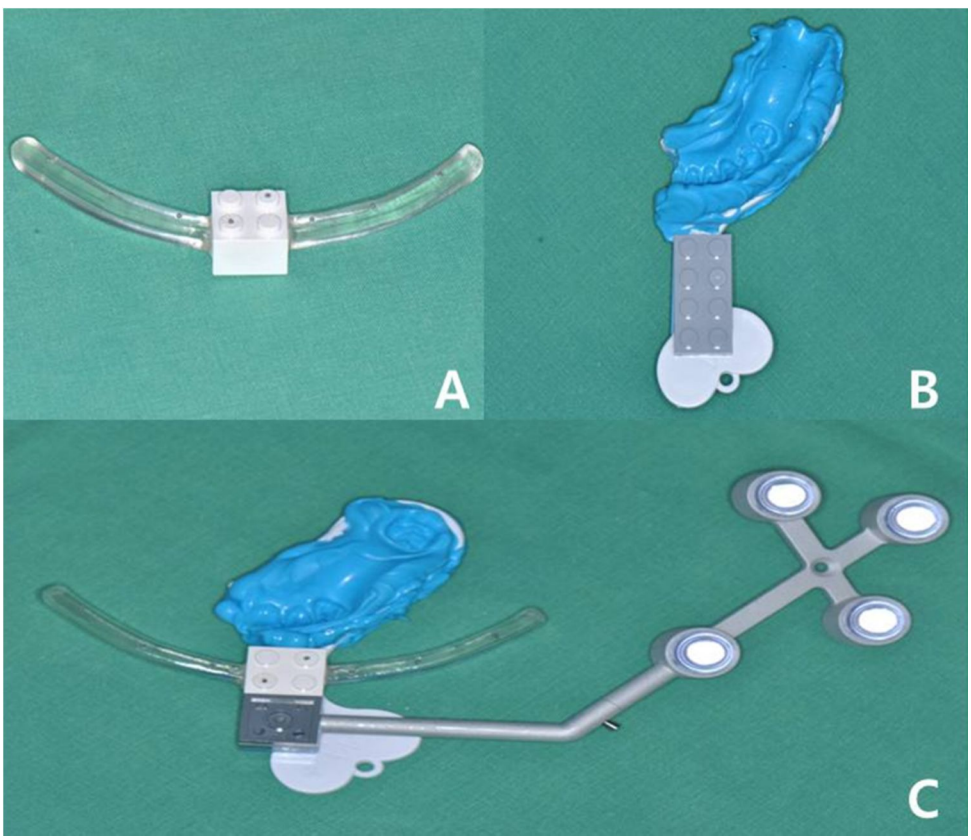

Fig. 4. A. The registration body is an arched frame composed of clear orthodontic self-curing acrylic resin with 8 ceramic spheres. B. A patient-specific splint is improvised by using a bite splint. C. The registration body and the patient tracking tool are attached to a splint by using a LEGO block.

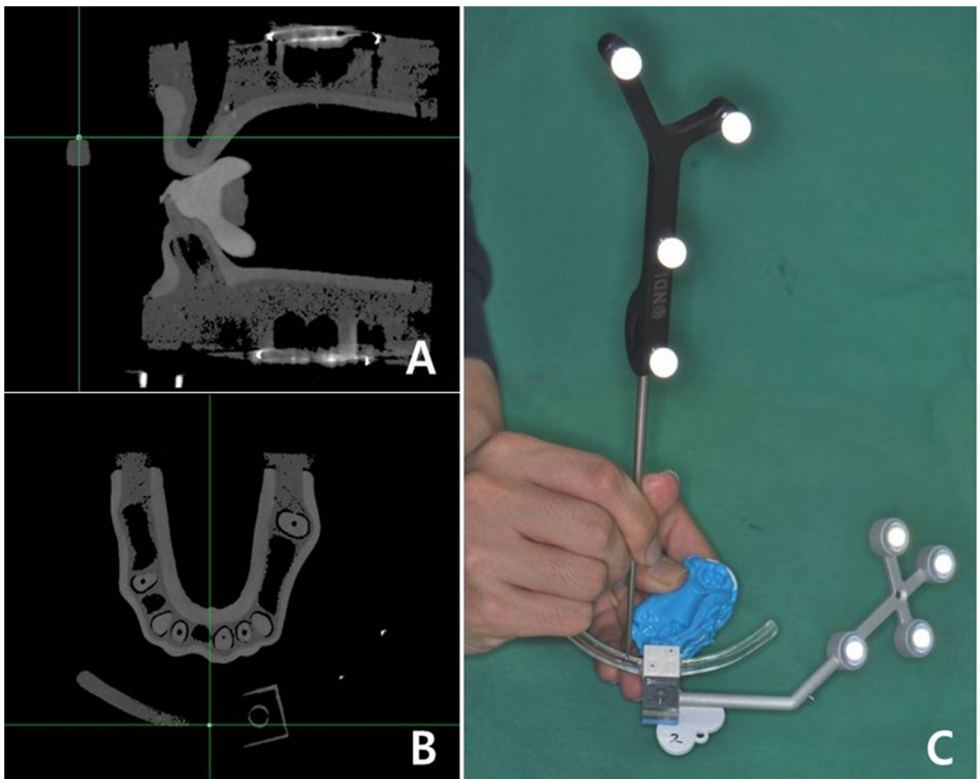

Fig. 5. A, B. the locations of the spheres in CBCT images. C. The locations of the physical positions of the sphere on the registration body is pointed by applying a tracked pointing tool.

Fig. 6. The offset vector of a new drill tip is determined by touching a point with the drill tip point and by pressing a foot-switch.

Fig. 7. A model has 10 embedded 1 mm diameter ceramic spheres (arrow) as targets.

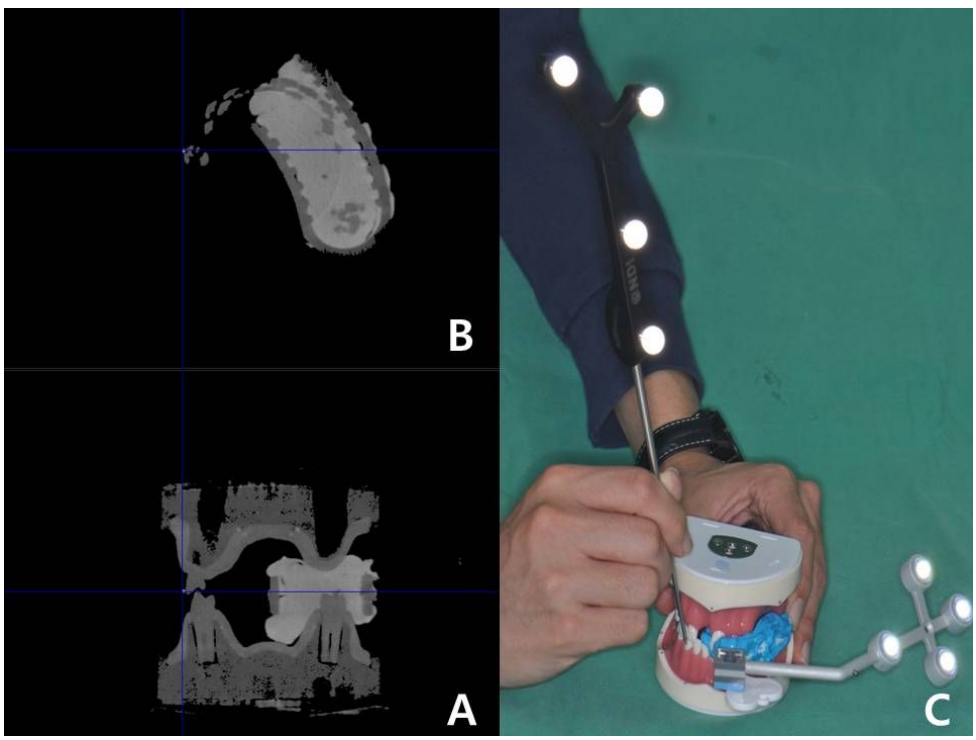

Fig. 8. A, B. The true position of the spheres in CBCT images. C. The physical location of the ceramic spheres is localized by using a tracked pointing tool. The root mean square (RMS) difference between true and tracked positions in the image for 10 landmarks was quantified as a registration error.

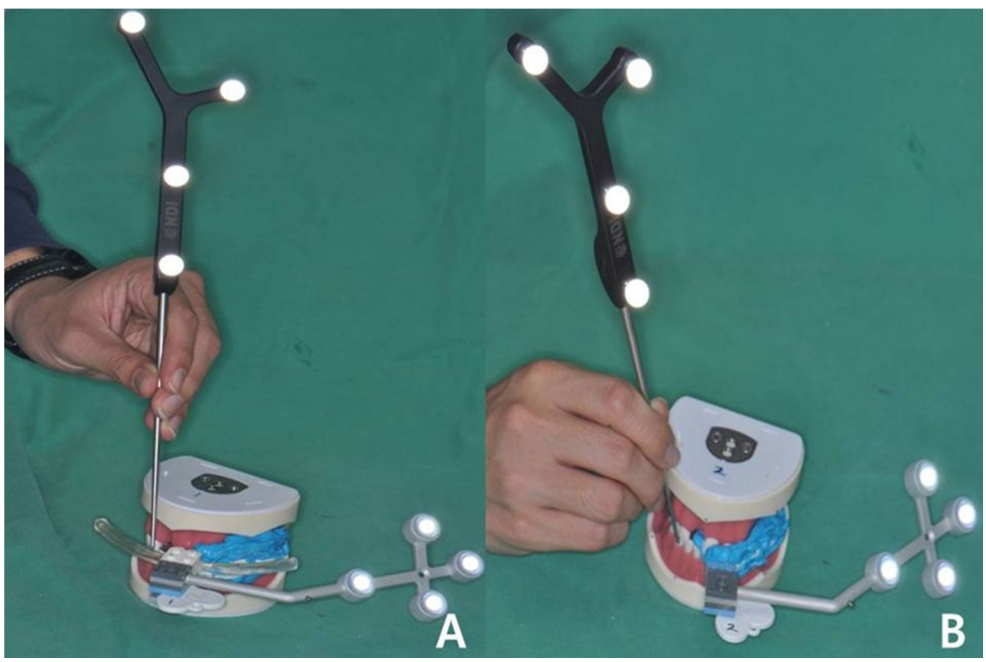

Fig. 9. A. Pre-recording of the physical positions of fiducials in a model. B. TRE measurement of the ceramic spheres after registration between the pre-recorded physical positions and image positions on another model.

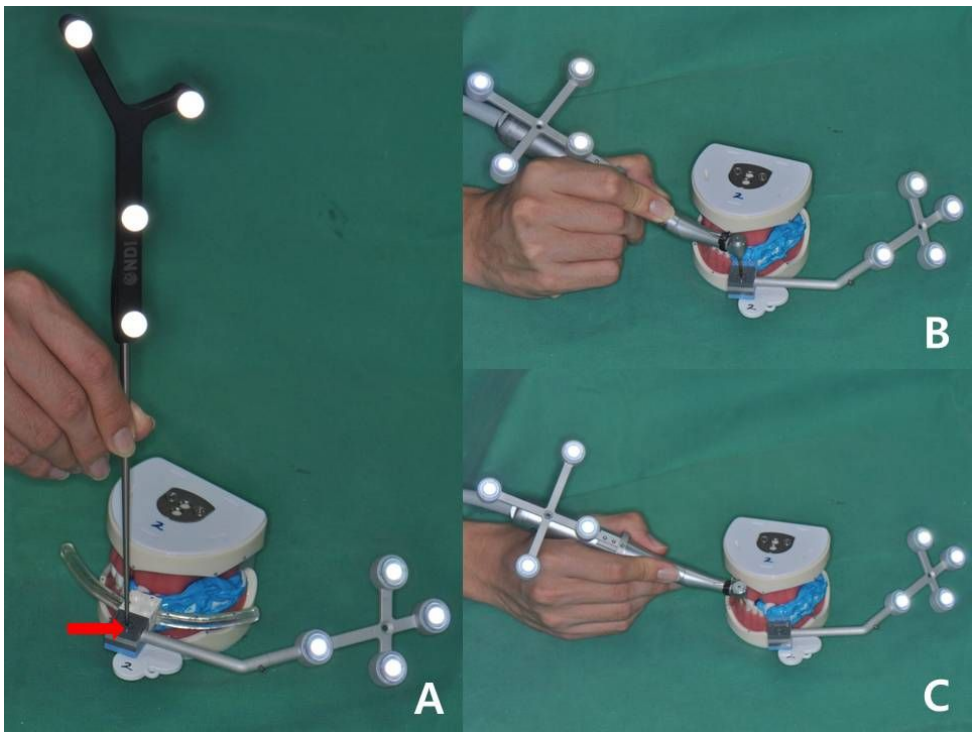

Fig. 10. A. Measurement of the landmark (arrow) coordinates by using the tracked pointing tool. B. The drill offset is automatically calculated from the obtained coordinates. C. By using this offset, the TRE of each ceramic sphere in a model is measured.

Fig. 11. A partially edentulous model.

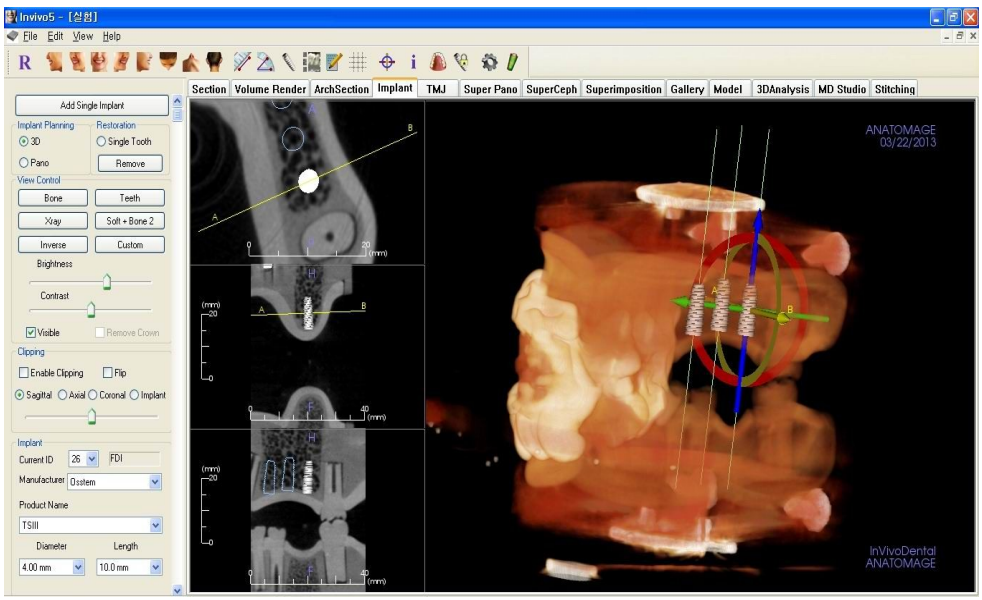

Fig. 12. Preoperative implant planning with the InVivoDental software.

Fig. 13. Implant placement by using the developed navigation surgery system. During a flapless procedure, the developed navigation surgery system provides the relative location of the drill in real time on the CT images.

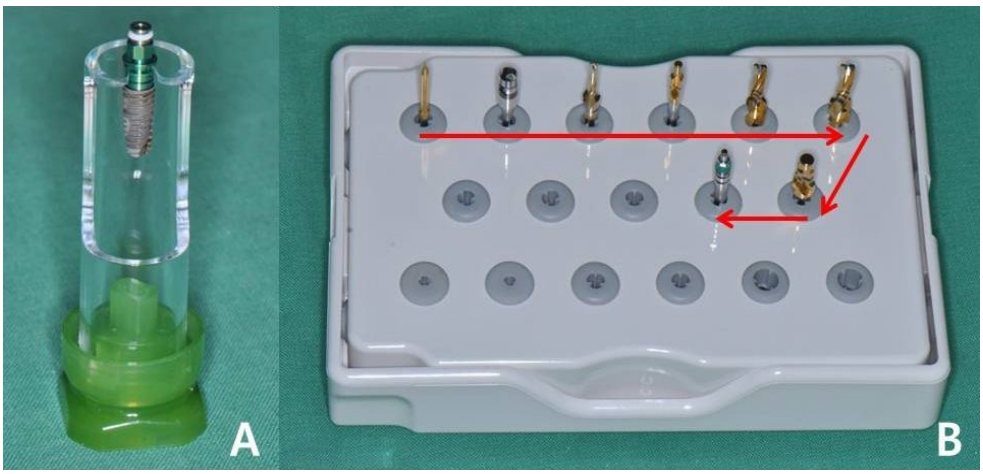

Fig. 14. A. The Osstem TS III implant. B. The drilling sequence of an implant socket. Arrows show the drilling order.

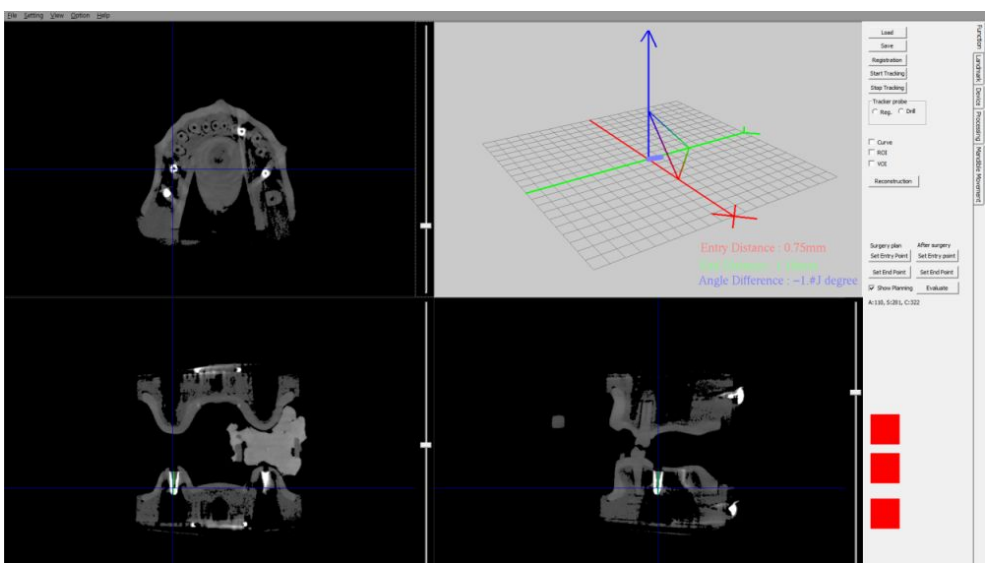

Fig. 15. The post-operative CBCT image is registered with the pre-operative CBCT image by point-to-point matching of the fiducial positions used in registration.

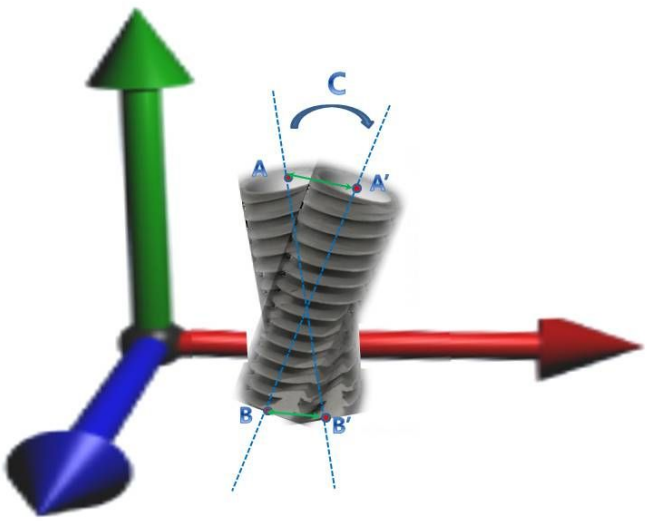

Fig. 16. A detailed method for measuring the deviations between planned and placed implants: the center point of the planned implant at the platform (A); the center point of the planned implant at the apex (B); the center point of the placed implant at the platform (A'); the center point of the placed implant at the apex (B'); angular deviation (C).

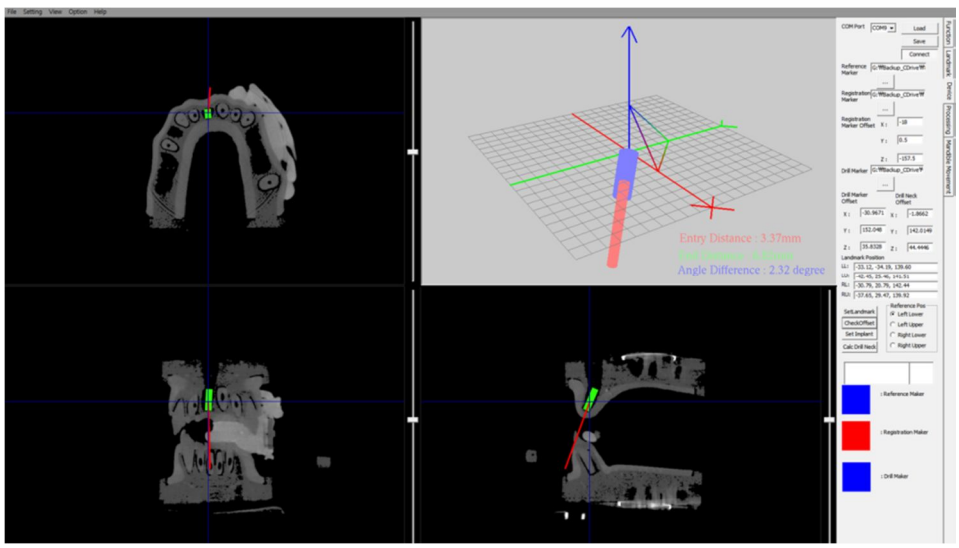

Fig. 17. An intraoperative screen of the navigation system. The positional difference between the location of drill tip and planned position of implant is quantified and visualized on the 3D view in real-time.

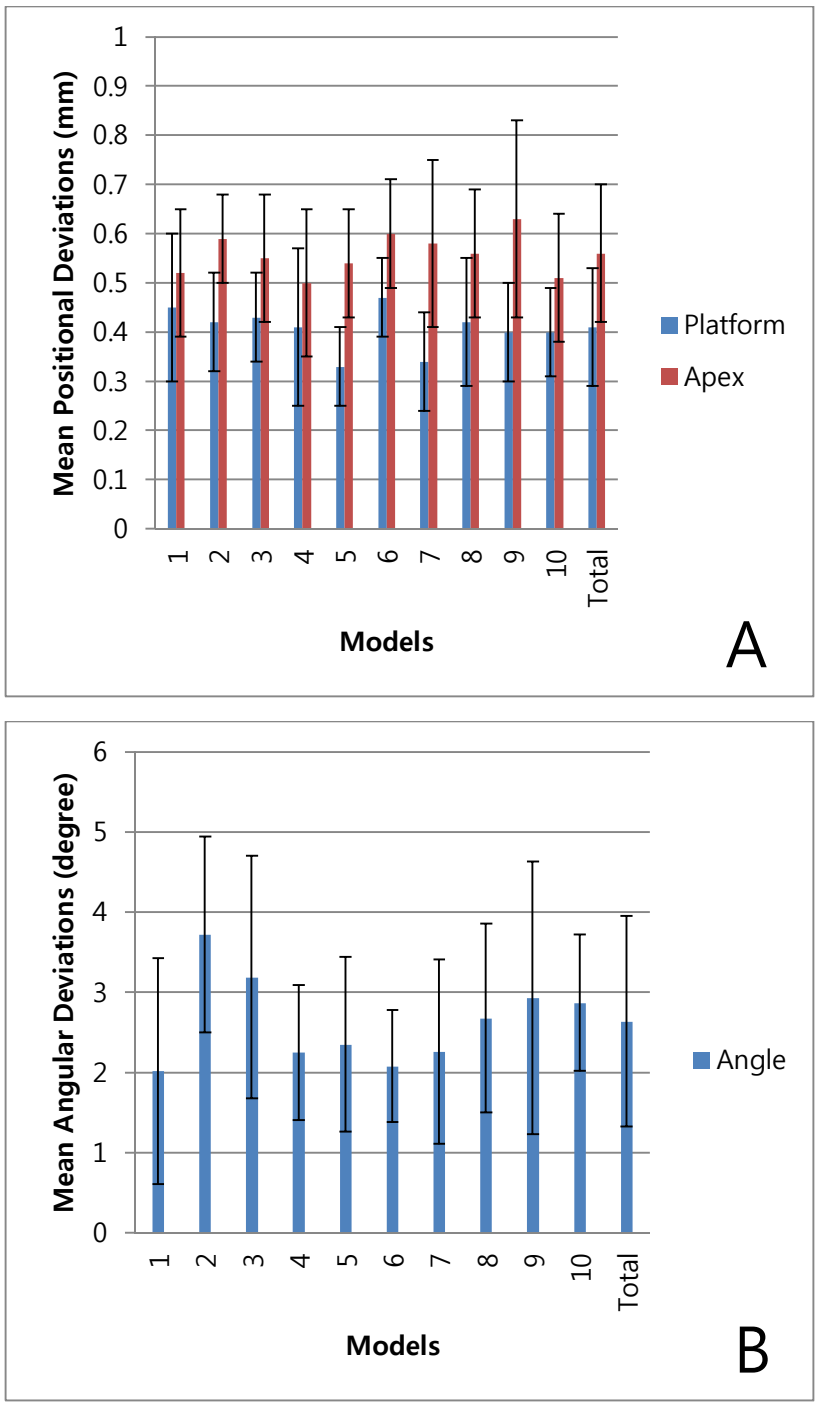

Fig. 18. A. The RMS accuracy (mean error) between planned and placed implants at the platform and the apex. B. The mean angular deviations according to the model.

국문초록

즉시 적용 가능한 치과 임플란트 수술용 영상유도 수술 시스템의 개발 및 평가

김 성구

서울대학교 대학원 치의과학과 구강악안면방사선학 전공

(지도교수 이원진)

1. 목 적: 본 연구의 목적은 콘빔전산화단층영상을 기반으로 한 새로운 치과 임플란트 수술용 영상유도 네비게이션 시스템을 개발하고, 시스템의 정확도를 평가하는 것이다.

2. 방 법: 본 연구에서는 광학적 위치추적 카메라를 기반으로 한 영상유도 수술 시스템을 개발하였다. 개발된 시스템에서는 새로운 기구 추적 장치 및 환자 추적 장치를 적용하였으며, 치과용 인상재와 바이트 트레이를 이용하여 환자용 스플린트를 즉시 적용 가능하게 하였다. 또한, 등록용 표지자의 물리적 좌표를 미리 저장하는 정합 방법과 자동적인 핸드피스의 오프셋 측정법을 개발하였다. 새로운 정합방법과 자동적인 핸드피스의 오프셋 측정법의 정확도를 10개의 지름 1mm 세라믹 구슬의 target registration error(TRE)로 측정하였다. 그리고,

임플란트 식립을 위한 영상유도 네비게이션 시스템의 오차를 측정하기 위해 실제 110개의 임플란트를 식립하여 개발된 시스템의 정확도를 평가하였다.

3. 결 과: 새로 개발된 시스템의 전체 평균 TRE는 0.35 ± 0.11 mm 를 나타냈다. 등록용 표지자의 물리적 좌표를 미리 저장하는 정합 방법을 시행한 후 TRE의 전체 평균은 0.34 ± 0.18 mm 를 나타냈다. 임의의 드릴의 offset을 자동으로 구한 다음 TRE의 전체 평균은 0.35 ± 0.16 mm 를 나타냈다. 방법 간 정확도의 유의한 차이는 존재하지 않았다. 110개의 계획된 임플란트와 실제 식립된 임플란트 간의 전체 평균 오차는 platform의 중심점에서 0.41 ± 0.12 mm, apex의 중심점에서 0.56 ± 0.14 mm, 임플란트 장축간의 각도 차이는 2.64 ± 1.31 ° 를 나타냈다.

4. 결 론: 기존 방법의 일부 단점을 극복하기 위해 콘빔 전산화 단층 영상을 기반으로 한 새로운 영상유도 임플란트 시스템을 개발하였다. 그리고, 시스템의 정확도는 임상적으로 충분히 사용 가능한 결과를 나타냈다. 따라서, 새로 개발된 영상유도 시스템을 적용하면 당일 즉시 임플란트 식립이 가능할 것으로 보인다.

주요어: 영상 유도 수술; 네비게이션 수술; 치과 임플란트; 콘빔전산화단층촬영, 즉시 임플란트

학 번: 2008-31042